# A Model that Explains the Contrasting SST Trends in the Southern Pacific Ocean

## Jialu Wang [1,a,*], Kaihuai Deng [2,b]

[1] *School of Atmospheric Sciences, Nanjing University of Information Science & Technology, Nanjing, China*
[2] *Longshan Academy, Nanjing University of Information Science & Technology, Nanjing, China*
*a. 202183300002@nuist.edu.cn, b. 202383300365@nuist.edu.cn*
*\*corresponding author*

**Abstract:**

Sea surface temperature (SST) of the southern Pacific Ocean plays an important role in ocean-atmospheric interactions, influencing both regional and global climate and ecosystems. The contrasting SST trends in the southern Pacific Ocean during 1993-2021 are noted by analyzing satellite and in-situ datasets, consisting of SST warming trend ($0.05°C·yr^{-1}$) in the region of 80°W-180,30°S-50°S and cooling trend ($-0.04°C·yr^{-1}$) in the area of 60°W-150°W, 55°S-70°S. A detailed trend analysis for the wind and sea ice concentration suggest that Ekman transport and sea ice radiative positive feedback are the two key contributors to the contrasting SST trends. The intensified downwelling (upwelling), induced by the Ekman transport and strengthened westerlies, gives rise to warm (cold) water swarming in (upturning) from lower latitudes (deeper ocean), which causes SST warming (cooling). Moreover, the sea ice increase at higher latitudes, due to both the cold water transport from deeper ocean layers and broken ice transport from polar regions, strengthens the cooling trend through sea ice positive radiative feedback. In conclusion, these findings underscore the complexity of SST trends in the southern Pacific Ocean, highlighting the critical roles of Ekman transport and sea ice radiative feedback in shaping regional climate dynamics.

Plain Language Summary: The southern Pacific Ocean is an indispensable part in the climate system while it still remained poorly observed. The SST trend is regarded as a critical indicator of global climate change. Using the satellite and in-situ datasets, we find that the contrasting SST trends from 1993 to 2021, one area in this region is warmed by 0.3℃ per decade, while another area is cooled by -0.1℃ per decade. Considering impacts of various factors such as wind, sea ice and radiation, the primarily explanation is that wind-driven warm (cold) water from the subtropics (deeper ocean) flows in and goes downward (goes upward and flow away) in the warm (cold) area through oceanic circulation and leads to the SST warming (cooling). Additionally, the cooling trend is also related to the cold water that flows to higher latitudes and forms ice there and at the same time, trash ice from polar regions driven by enhanced south wind speed will be transported there. As a result, ice increases, reflects more shortwave radiation to space, and surface downward shortwave radiation decreases which contributes to SST decreases.

**Keywords:** SST trends; Ocean-Atmoshpere-Ice Interaction; the Southern Pacific Ocean

## 1. Introduction

Understanding sea surface temperature (SST) is of great significance for enriching our understanding of ocean-atmospheric interactions and global climate dynamics (Kieu et al., 2023). The South Pacific Ocean (60 °W-180,70°S-30°S) serves as a major heat reservoir and plays a crucial role in regulating global climate. It stores and redistributes vast amounts of heat and therefore significantly impacts global climate system. (Jones & Ricketts, 2021; Li et al., 2022) By influencing ocean heat content on interannual to decadal timescales, wind-driven ocean circulation functions as a regulator of the Earth's energy balance (Fernandez et al., 2022). SST variations in the South Pacific can significantly affect regional climate, particularly in areas like New Zealand. Studies have shown that SSTs around New Zealand are correlated with barotropic Rossby waves estimated from South Pacific wind stress (Bowen et al., 2017). Recent studies have highlighted the impact of climate change on SST trends in the South Pacific. Observations indicate a persistent trend toward enhanced east-west and north-south SST gradients, which are believed to be

responses to radiative forcing rather than internal variability (Seager et al., 2022). Furthermore, the change of SST is closely related to the ecosystem of the local sea area. For example, SST distribution is critical to shaping seabird assemblages across the Eastern South Pacific Ocean by significantly influencing their abundance and species richness as indicators of ocean productivity (Serratosa et al., 2020). Thus it is noted that understanding SST variations and their interactions with oceanic and atmospheric processes is crucial for predicting regional climate impacts and assessing long-term climate change effects in the South Pacific.

Recently, the trend of SST has attracted much attention, and the underlying reasons have also been studied. A positive trend in temperature was recorded in an area of the ocean situated around 179°E, 46°S, which suggests a notable increase in sea surface temperatures over recent decades, showing that the warming is a result of changes in the local flows of Subantarctic Water (Sutton et al., 2024). These changes led to the relocation of sea ice away from the Antarctic coast and exposed the ocean beneath to solar radiation, thereby warming the water mass and accelerating the melting of sea ice. Another contributing factor might be the exceptionally stronger southwesterlies, which drove the sea ice drifting away from this basin and toward the east (Turner et al., 2022). Meanwhile, Saurral highlighted that the increasing SST trend in the South Pacific region is associated with sea level pressure and surface advection (Saurral, 2018).

Apart from the warming feature, Haumann identified a cooling pattern in the region between the ice edge and the subantarctic front in the Pacific sector from 1982 to 2011. This cooling trend was found to be closely associated with changes in sea ice (Haumann et al., 2020). There were other meteorologists discovering that changes in the net surface shortwave radiation and Ekman horizontal advection are the two key factors to the SST cooling (Xu et al., 2022).

However, the mechanism under the SST warming and cooling of the two areas has not been thoroughly studied. The interaction between these contrasting temperature trends and their driving forces remains unclear, posing a challenge for understanding the regional climate dynamics.

This study aims to investigate the SST warming and cooling trends in the southern Pacific Ocean, and reveal the sea-air-ice interaction mechanisms, which dominate the SST variability. The structure of this document is as follows. Section 2 presents the study's data and methodology. Section 3 examines the patterns and processes of SST variability related to physical surroundings. Lastly, Section 4 provides a summary of our main conclusions.

## 2. Data and Methods

The data products described below were used to define and analyze the ocean changes. The datasets were collated in tabular form for enhanced clarity.

**Table 1. Overview of variables, timescale, resolution and source. In order to maintain consistency and control variability, the majority of the datasets were collected between 1993 and 2021.**

| Type | Variable | Time | Resolution | Source |
|---|---|---|---|---|
| Satellite Data | SST | 1993~2021 | 0.05° × 0.05° | Copernicus |
| | SSH | 1993~2021 | 0.25° × 0.25° | DUACS |
| | Radiation | 2001~2021 | 1° × 1° | CERES |
| Reanalysis Data | SLP | 1993~2021 | 2.5° × 2.5° | NCEP |
| | SSW | 1993~2021 | 2.5° × 2.5° | NCEP |
| | SIC | 1993~2021 | 25 km × 25 km | NSDIC |

## 2.1 Satellite Data

### 2.1.1 Sea Surface Temperature

For this study, we calculated the monthly SST trends for the period from 1993 to 2021. The data employed in this study is extracted from the Copernicus objectively analyzed sea surface temperature (SST) product. This product is based on daily, global climate SST analyses generated by the European Space Agency (ESA) SST Climate Change Initiative (CCI) and the Copernicus Climate Change Service (C3S) (product SST-GLO-SST-L4-REP-OBSERVATIONS-010-024) (Merchant et al., 2019). The data provides a comprehensive and consistent dataset for climate analysis and is available at https://doi.org/10.48670/ moi-00243 (Last accessed: 3rd August 2024).

### 2.1.2 Sea Surface Height

The data utilized in this study, namely the daily sea surface height (SSH), is sourced from the delayed time (DT-2021 version) SSH maps provided by the DUACS, spanning the period from 1993 to 2021. This dataset is sourced from the Copernicus Climate Change Service and the Copernicus Marine Service (product SEALEVEL_GLO_PHY_CLIMATE_L4_MY_008_057) and combines the available multi-year dataset and the multi-year interim dataset. The dataset is based on a fixed number of altimeters in the aforementioned satellite constellation, thereby guaranteeing consistent and reliable sea level observations. More details about the product can be found at https://doi.org/10.48670/moi-00238 (Last accessed: 3rd August 2024).

### 2.1.3 Radiation

The dataset employs CERES EBAF(Energy Balanced and Filled) data, SYB1deg - Level 3, from NASA/LaRC (Kato et al., 2018; Loeb et al., 2018), which were recorded on a monthly basis from 2001 to 2021. The Climate Data Record (CDR) encompasses monthly and climatological mean values of observed and calculated surface all-sky, clear-sky (spatially exhaustive), and cloud radiative effect (CRE) fluxes, along with associated clouds. It is suitable for the analysis of intra-seasonal, inter-annual, and longer-term variability. The TOA net flux is defined in terms of ocean heat storage. CERES can be found at https://ceres.larc.nasa.go (Last accessed: 3rd August 2024).

## 2.2 Reanalysis Data

### 2.2.1 Sea Level Pressure

We utilized the NCEP-NCAR Reanalysis data (provided by the NOAA PSL, Boulder, Colorado, USA, from their website at https://psl.noaa.gov, Last accessed: 27th September, 2024) to analyze sea level pressure (SLP) trends from January 1993 to December 2021. The comprehensive dataset is developed by the National Centers for Environmental Prediction (NCEP) and the National Center for Atmospheric Research (NCAR) together (Kalnay et al., 1996). It offers global coverage at a spatial resolution of 2.5° × 2.5°. The reanalysis data covers the period from 1948 to present, integrating a wide array of meteorological variables assimilated by a consistent model. The enduring consistency and worldwide coverage of this dataset make it exceptionally valuable for investigating climate trends and variability.

### 2.2.2 Sea Surface Wind

The NCEP-NCAR Reanalysis dataset was utilized to analyze trends in sea surface wind speed (SSW) from January 1993 to December 2021. In this study, monthly SSW com-ponents (U, V, and W) were extracted for trend analysis. It was also employed for the SLP. By using the identical dataset for both wind speed and pressure analyses, coherence in the findings was ensured, allowing exploration of potential relationships between these atmospheric variables over a period of nearly three decades.

### 2.2.3 Sea Ice Concentration

The ice concentration data were obtained from the National Snow and Ice Data Center (NSIDC) (Meier et al., 2021) and are measured on a monthly basis, available on a 25 km × 25 km grid. This dataset constitutes a Climate Data Record (CDR) of sea ice concentration derived from passive microwave observations. The CDR algorithm integrates ice concentration estimates by employing a rule-based approach and combining outputs from two established algorithms: the NASA Team (NT) algorithm (Cavalieri et al., 1984) and the NASA Bootstrap (BT) algorithm. Detailed information about the dataset and access to the data can be found at https://doi.org/10.7265/EFMZ-2T65 (Last accessed: 3rd August 2024).

## 2.3 Methods

Univariate Linear Modeling: To analyze the trends in SST, SSH, Radiation, SLP, SSW and SIC in the Southern Ocean, we utilized univariate linear modeling. In statistics, regression analysis is adopted to identify the relationship between a dependent variable and another. In this study, we applied the technique to determine the rates of change in SST and SLA over the period from 1993 to 2021.

For each grid point within the study regions, we performed a linear modeling analysis to estimate the trend over the approximately 30-year period. The linear model is defined as:

$$Y = \beta_0 + \beta_1 X + \epsilon \tag{1}$$

Where Y is the variables, X is time (in years), $\beta_0$ is the intercept, $\beta_1$ is the slope (trend), and $\epsilon$ is the error term. The rate of change in variable per year is represented by the slope $\beta$.

Ekman Mathematical Derivation: The Ekman mathematical derivation (Cushman-Roisin & Beckers, 2011) was employed to calculate wind induced water flow in the zonal, meridional and vertical directions, with a view to establishing a wind trend in the southern hemisphere.

$$UE = -\frac{T_y}{\rho_w f} \, , \, ?VE = -\frac{T_x}{\rho_w f} \, , \, WE = \frac{1}{\rho_w f}\left(\frac{\partial T_y}{\partial x} - \frac{\partial T_x}{\partial y}\right) \tag{2}$$

Where UE, VE and WE represent Ekman transport in the $u$, v and w direction. $T$ is the wind stress, $\rho$ is the density, $f$ is the Coriolis parameter, constant. In the UE and VE equation the plus sign applies to the northern hemisphere and the minus sign to the southern hemi-

sphere. (Cushman-Roisin & Beckers, 2011)

# 3. Results

## 3.1 Linear trends of SST, SSW, SLP, SIC and SSH

Figure 1 shows the linear SST trend in the southern Pacific Ocean(80 °W-180,70°S-30°S). The SST trend reveals a contrasting pattern in the study region. The warming region (80 °W-180,50°S-30°S) , located in the South Pacific Ocean, exhibits an overall increasing trend of approximately 0.3°C·decade$^{-1}$, with a maximum warming rate reaching up to 0.6°C·decade$^{-1}$. Conversely, the cooling region is found at the area of 150 °W-60°W,70°S-50°S, where shows an average decreasing trend of about

-0.1°C·decade$^{-1}$, with the maximum declining rate reaching -0.2°C·decade$^{-1}$.This pattern is consistent with findings from previous studies. A recent study (Sutton et al., 2024) have documented similar warming trends in the South Pacific Ocean, indicating a significant increase in SSTs in recent decades. The cooling trend observed aligns with the previous results , identifying a similar cooling pattern in the region between the ice edge and the subantarctic front in the Pacific sector from 1982 to 2011 (Haumann et al., 2020). However, our findings suggest that the SST exhibits the contrasting trend changes in the study region. Thus, the warming area connected to co-occurring cooling needs more mechanism discussion.
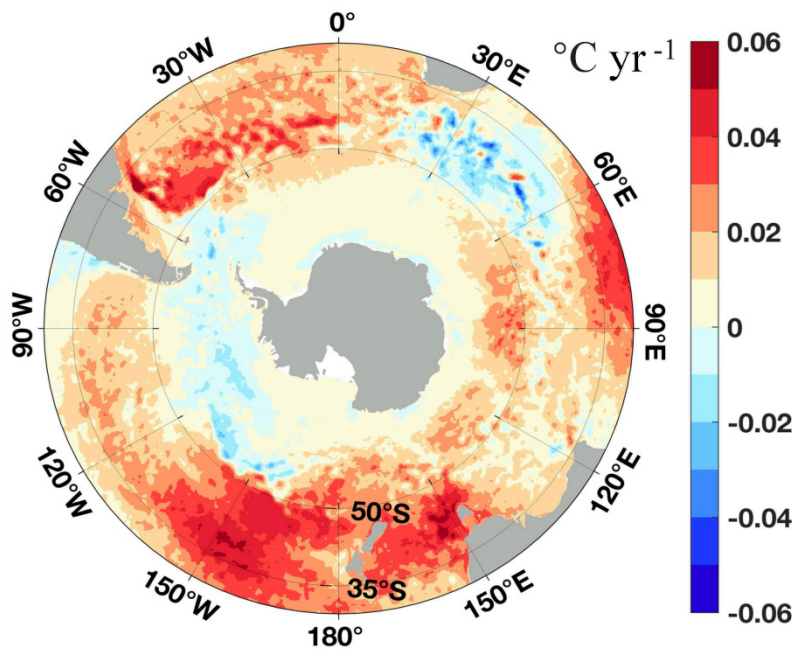


**Figure 1. Sea surface temperature annual trends distribution in the Southern Hemisphere during 1993-2021 (°C yr$^{-1}$ ). The studied warming region is in 80°W and 180°W, 50°S and 30°S. The cooling region is 60°W and 150°W, 70°S and 55°S. (The dotting area is statistically significant at 95.5% confidence level by Student's t-test.)**

Simultaneously, other variables (i.e., SSW, SLP, SSH and SIC) exhibit significant anomalies trends across the regions (Figure 2). In the warming region (80 °W-180,50°S-30°S), the SSW shows a reduction in wind speed with a trend of -0.03m·s$^{-1}$·decade$^{-1}$. The SLP, indicates an upward trend of 0.65 millibars·decade$^{-1}$. Regarding the SSH, the warming region demonstrates a rising trend of 50mm·decade$^{-1}$. In general, the warming region exhibits a

tendency towards deceleration in sea surface wind speed, an increase in sea level pressure and an elevation in sea surface height. While for the cooling region(60°W-150°W, 55°S-70°S), the SSW displays an ascending trend of 0.02m·s$^{-1}$·decade$^{-1}$. For SLP, a decreasing trend was shown in -1.95 millibars·decade$^{-1}$. The SSH in the cooling region exhibits a declining trend of -20mm·decade$^{-1}$. To conclude, the cooling region displays a pattern of increasing

sea surface wind speed, a reduction in sea level pressure and a decline in sea surface height.

The sea ice concentration (SIC) shows an incremental trend in the band of 65°S − 70°S, 90°W − 150°W. While a trend toward decline in the band of 70°S − 75°S,120°W − 180 (See Section 3.3).
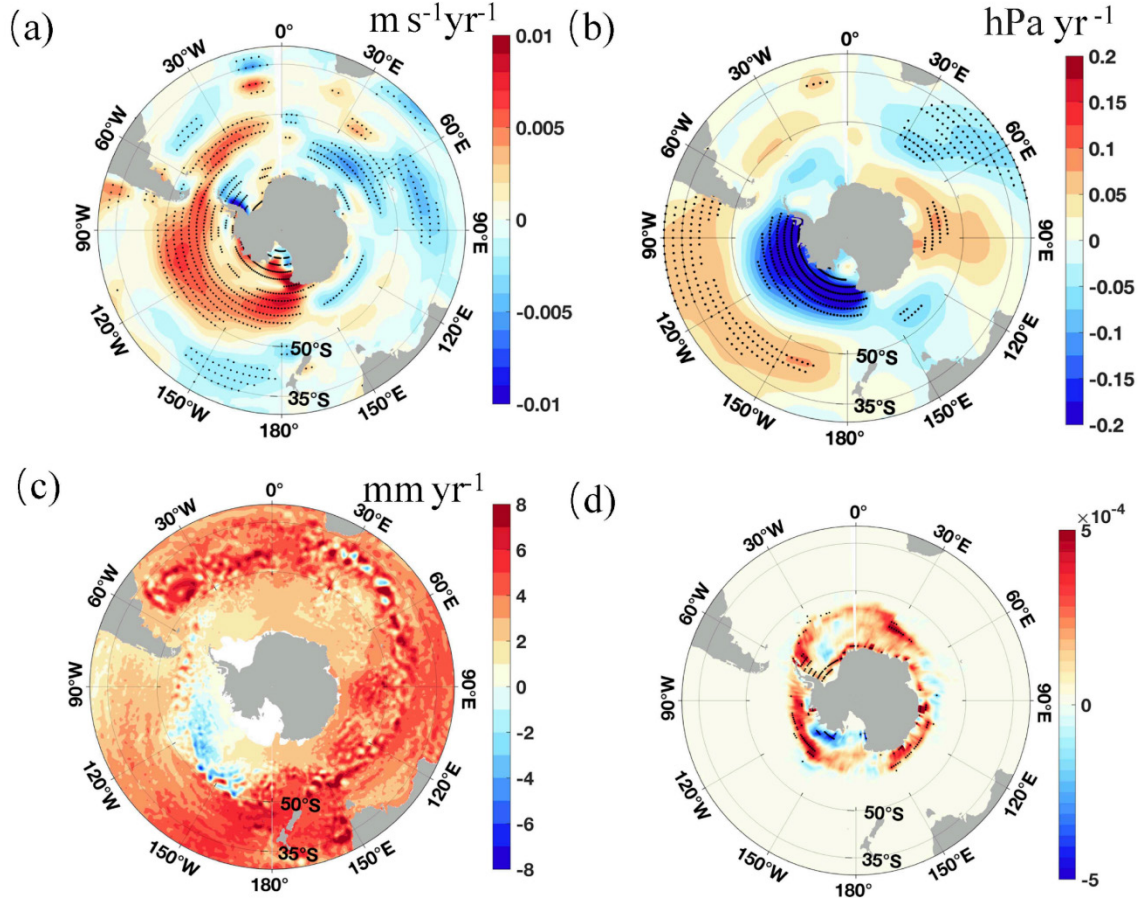


**Figure 2. Annual trends distribution of SSW, SLP, SSH and SIC in the Southern Hemisphere during 1993-2021. (a) The trend of SSW (m · s$^{-1}$ · yr$^{-1}$). (b) The trend of SLP (hpa · yr$^{-1}$). (c) The trend of SSH (mm·yr$^{-1}$). (d) The trend of SIC (% · yr$^{-1}$). (The dotted area is statistically significant at the 95.5% confidence level.)**

## 3.2 Underlying Mechanism for Ekman transport

Using Ekman mathematical derivation, we calculated the Ekman transport in the horizontal and vertical directions. The analysis, depicted in Figures 3a-c, illustrates the climatology of Ekman transport in zonal (UE), meridional (VE), and vertical (WE) directions. In the warming regions (80° W-180,50°S-30°S), zonal transports(u direction) exhibit a predominant positive pattern, indicating a dominant eastward transport. In the meridional direction (v), the meridional transports also show a significant positive tendency, suggesting a stronger northward transport. Additionally, the vertical direction (WE) displays a negative pattern, implying the downwelling processes. In the cooling regions (80°W-180,50°S-30°S), the zonal and meridional transports are similar to the warming area, but the intensity of the zonal and meridional transports is weaker than that of the warming region. Conversely, the significant negative Ekman pumping (WE) is found in the cooling region, which confirms the upwelling processes.

Figure 3d-f reveals the trend of Ekman transport patterns during 1993-2021.In warming regions (80°W - 180,50°S

- 30°S), the zonal transports exhibit a positive trend, indicating an increased tendency to blow eastward. In the meridional transport, there is a dominant positive tendency, with a stronger northward flow. Vertically, a significant negative trend is found, and related to the enhancing downwelling. At the same time, cooling regions display opposing trends, with a significant negative trend, highlighting the intensity of downwelling.
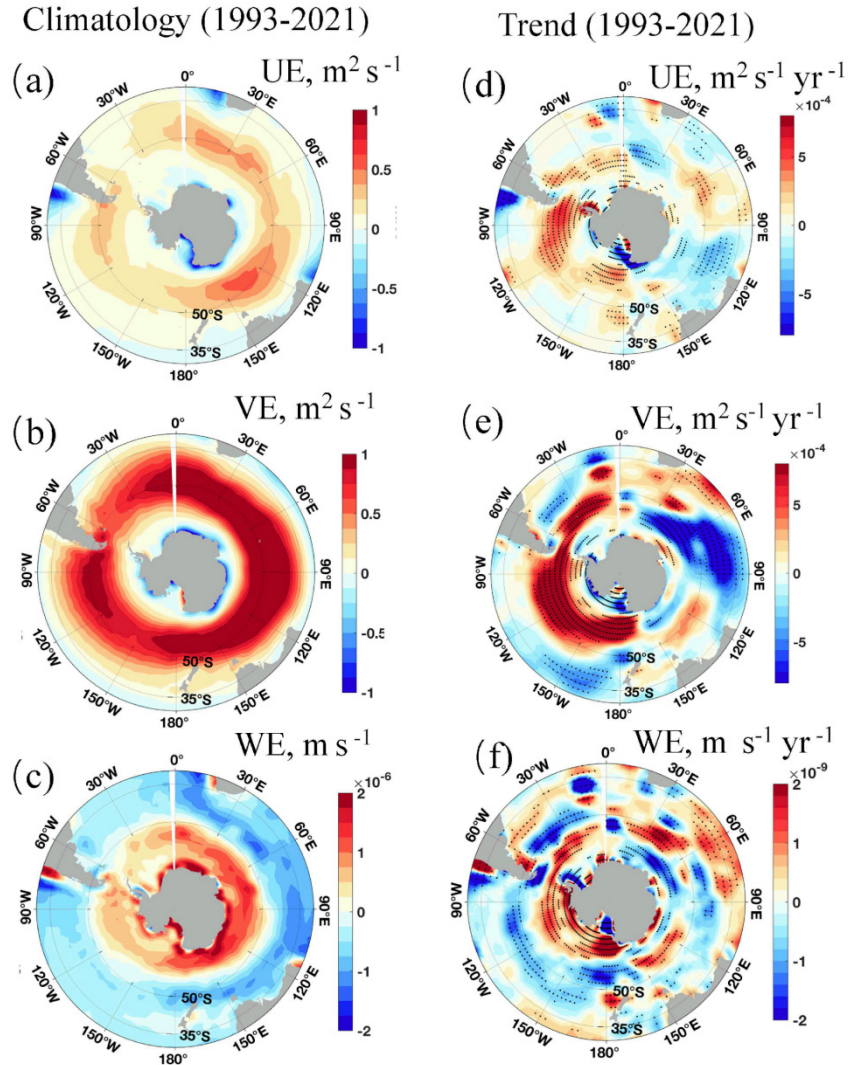


**Figure 3. The climatology and the annual trends distribution in zonal, meridional and vertical direction during 1993-2021. (a-c) shows the climatology distribution. (d-f) shows the trends distribution. (The dashed area is statistically significant at the 95.5% confidence level.)**

All in all, this consistency between climatological patterns and trends emphasizes the dominance of the Ekman transport in meridional direction, reinforcing the overall understanding of wind dynamics in the study region. The contrasting SST in the studied region is highly related to the Ekman transport. The strengthened downwelling (upwelling) induced by wind-driven convergence (divergence) process could be responsible for the warming (cooling) in the studied region.

## 3.3 More Possible Causes of SST Cooling

From the mechanism for Ekman transport between differ-

ent sea areas with contrasting SST trends, the intensified upwelling in the cooling sea area may bring cold water from subsurface ocean upward, which facilitates the ice formation near the Antarctic circle where the SST is always below 0 ℃. Therefore we focus on the area with sea ice coverage all year around in the Southern Ocean (65°S-75°S, 180°-90°W) (labeled Area 0) and its trend from 1993 to 2021 (Figure 4). And the assumption corresponds well with the real trend we observe, that the sea ice piles up significantly at the edge of the cooling area (65°S-70°S, 90°W-150°W) (labeled with Area 1), consist-

ing with previous study (Hobbs et al., 2016).
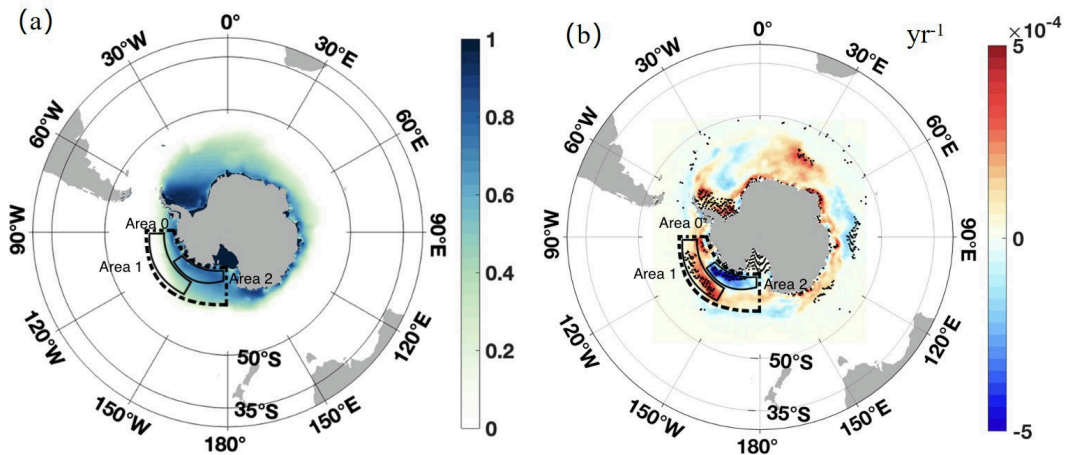


**Figure 4. The climatology(a) and the trends(b) distribution in sea ice concentration (SIC) (%·yr$^{-1}$) of Area 0,1,2 during 1993-2021. (The dotting area is statistically significant at 95% confidence level.)**

In order to figure out the contribution of sea ice to the cooling trend, we consider sea-ice radiative feedback contribution and thus we analyze the climate states and trends of the outgoing TOA shortwave flux, outgoing TOA longwave flux and TOA net downward radiation flux under clear sky in the Area 0 from 2001 to 2021 (Figure 5). For the edge of the cooling area, the Area 1, the observations show a positive trend in TOA shortwave flux whereas negative trends in both outgoing TOA longwave flux and TOA net downward radiation flux (Figure 5d-f). Taking their climate states into consideration (Figure 5a-c), we noticed that the Area 1 reflects more shortwave into extra-atmosphere, and loses more heat generally than before. Although the outgoing TOA longwave flux trend indicates that the cooling area radiates less longwave out, its slower speed leads to the dominant role of TOA shortwave flux, resulting in less and less heat storage and cooler SST. Subsequently, the lower temperature brings about more ice formation and accumulation and the sea-ice radiative positive feedback runs in cycles, which is a possible cause of cooling trend in the period of 1993-2021.
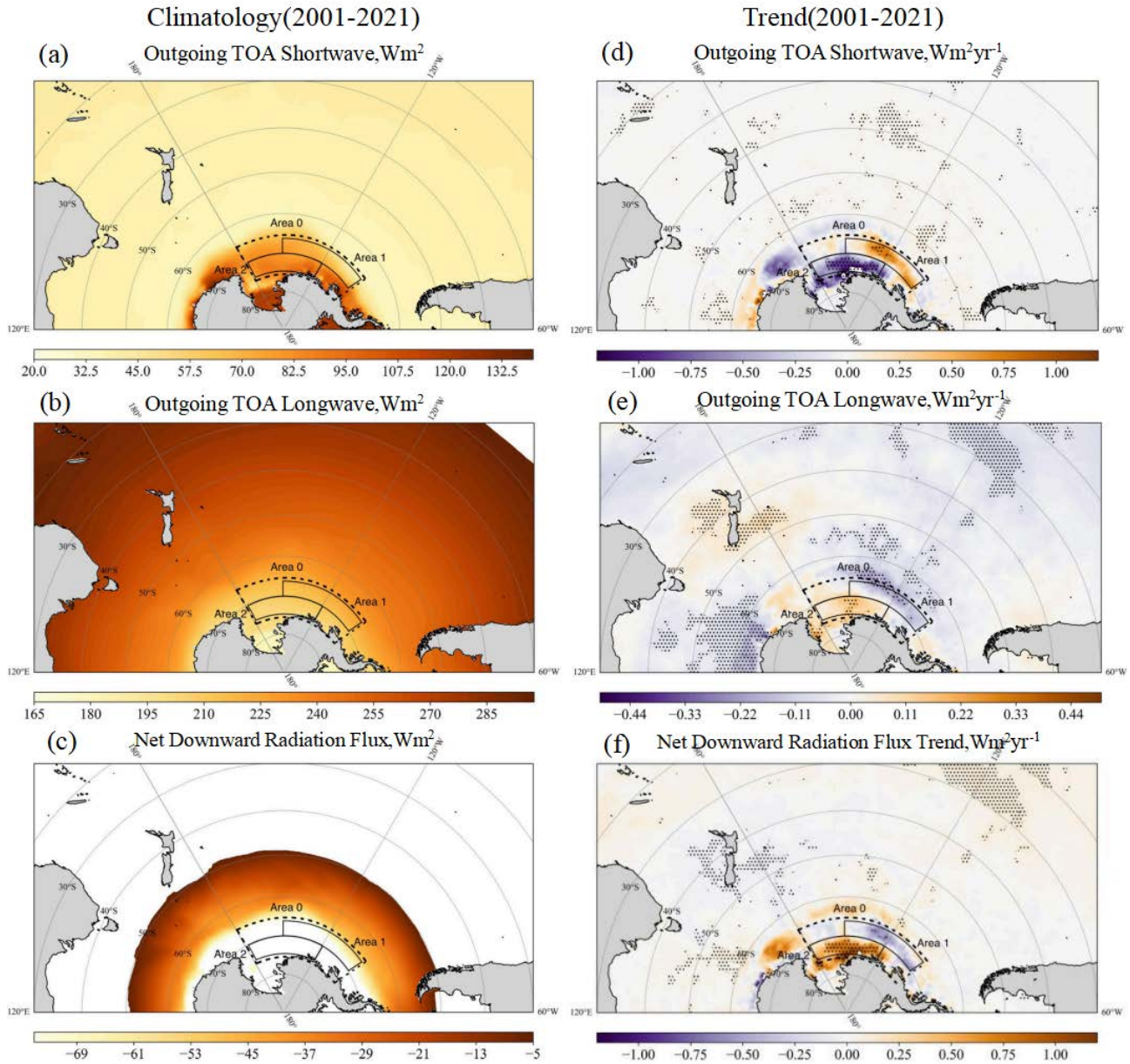
**Figure 5. The climatology(w·m⁻²) and the trend(w·m⁻²·yr⁻¹) distribution in outgoing TOA shortwave flux(a, d), outgoing TOA longwave flux(b, e) and TOA net downward radiation flux(c, f) under clear sky of Area 0,1,2 during 1993-2021 (The dashed area is statistically significant at the 95.5% confidence leve.)**

A striking new result is that the sea ice significant decline at higher latitudes(70°S-75°S,180°-120°W) (labeled with Area 2) than the edge of the cooling area (Area 1), contradicts with the principle that ice melts at lower latitudes with more heat. We examine the rea- sons and consequences of the ice loss in the Area 2 and find out the change of sea level pressure (SLP), controlling sea surface winds (SSW) strongly, is consistent with observations of change of ice concentration (Figure 6). A depression, which is called The Amundsen low, controls the almost southerly wind near the Ross Sea and the Amundsen Sea throughout the year (Figure 6a). Due to the intensifying depression over the period (Figure 6b), the south wind picks up (Figure 6c-d), speeds up the trash ice transport from Area 1 to Area 2, and the exposed sea surface gains more heat through sea-ice radiative positive feedback, which accelerates ice breaking and transport finally. That also accounts for the opposite trend in Area 2 of all radiation components mentioned above to Area 1. As a consequence, the sea ice decline at higher latitudes is a contrib-

utor to the sea ice accumulation and cooling trend in the cooling area.
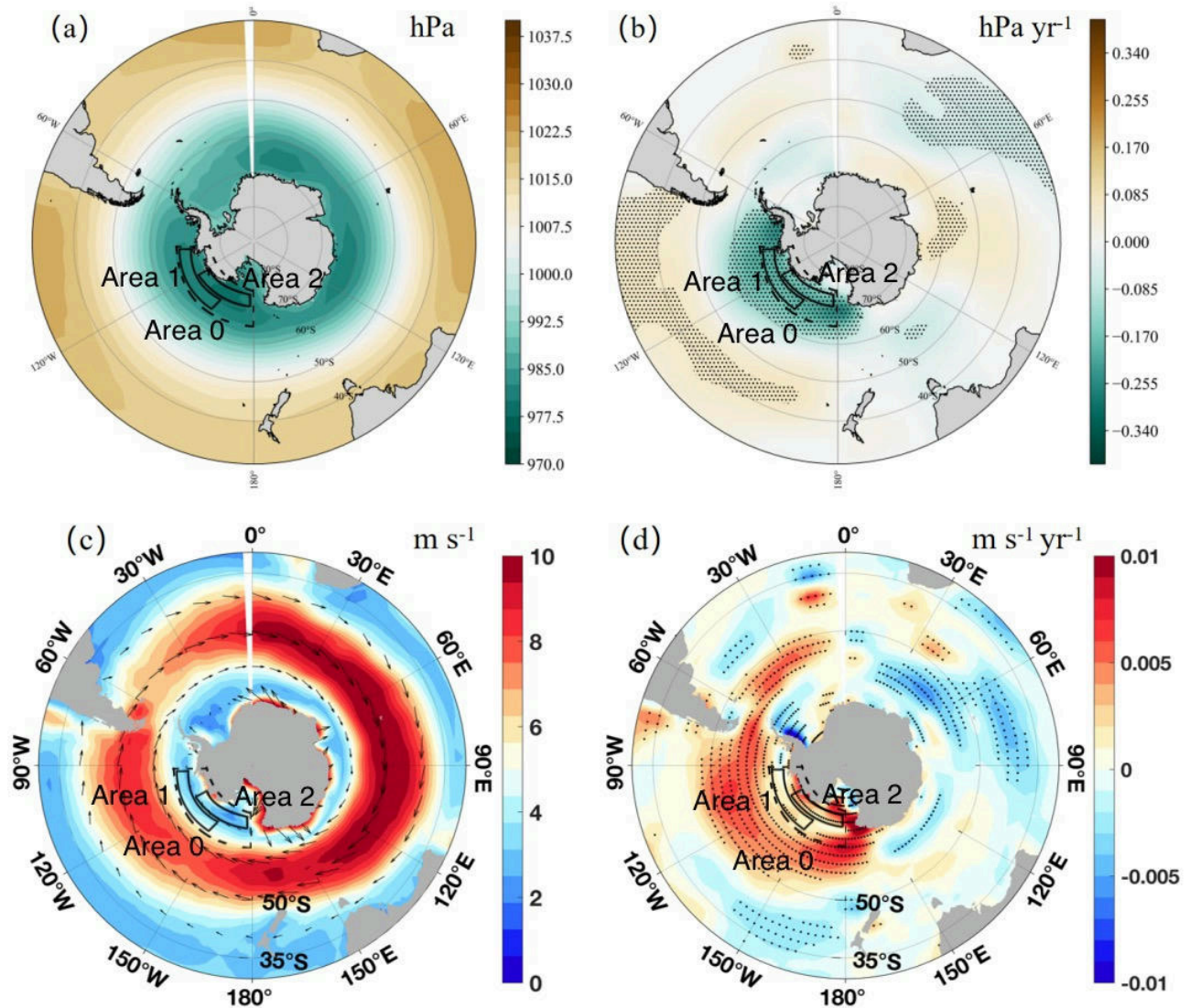


**Figure 6. The climatology and the trend distribution in sea level pressure (SLP) (a-b) and sea surface winds (SSW) (c-d) of Area 0,1,2 during 1993-2021 (The dotting area is statistically significant at 95% confidence leve.)**

## 4. Conclusions

To provide an overview of the main findings of this study, a conceptual model is presented in which illustrates how the sea-ice-air interactions explain the contrasting SST trends in the Southern Pacific Ocean (Figure 7). The concurrent SST warming and cooling trends at different latitudes are found in the Southern Pacific Ocean. Due to the strengthening and southward shift of the Southern westerlies, the intensifying upwelling (downwelling) at higher(lower) latitudes, induced by wind- driven Ekman transport, cloud be responsible for the cooling (warming) trend, which establishes a hydrological cycle for the movement of surface layer water. Moreover, sea ice radiative positive feedback plays a critical role in the SST descending. To be specific, cold water carried by local upwelling and sea ice transported by southeasterly winds contribute to a significant increase in sea ice in the cooling area, accelerating heat loss and further aggravating the cooling by reflecting more radiation out of the atmosphere. Accordingly, the cooling trend may persist for a while, along with progressively increasing SST differences, doing harm to the ecology and fishery resources of the Southern Pacific Ocean and exacerbating global climate instability and human society production in the future, which should be paid much attention to by public.

Some deficiencies in this study, however, should never be underestimated. On one hand, the uncertainties brought by data and methods could influence the dependability of the results. For example, errors will be brought in the process of satellite data retrieving and processing observations into reanalysis data. Moreover, the error term included in the linear regression model will affect the accuracy of the conclusions to some extent. On the other hand, some underlying mechanisms still remain unclear, such as the impacts of the seasonal cycle of sea ice concentration and the cloud radiative feedback, which would be fully implemented in the future.
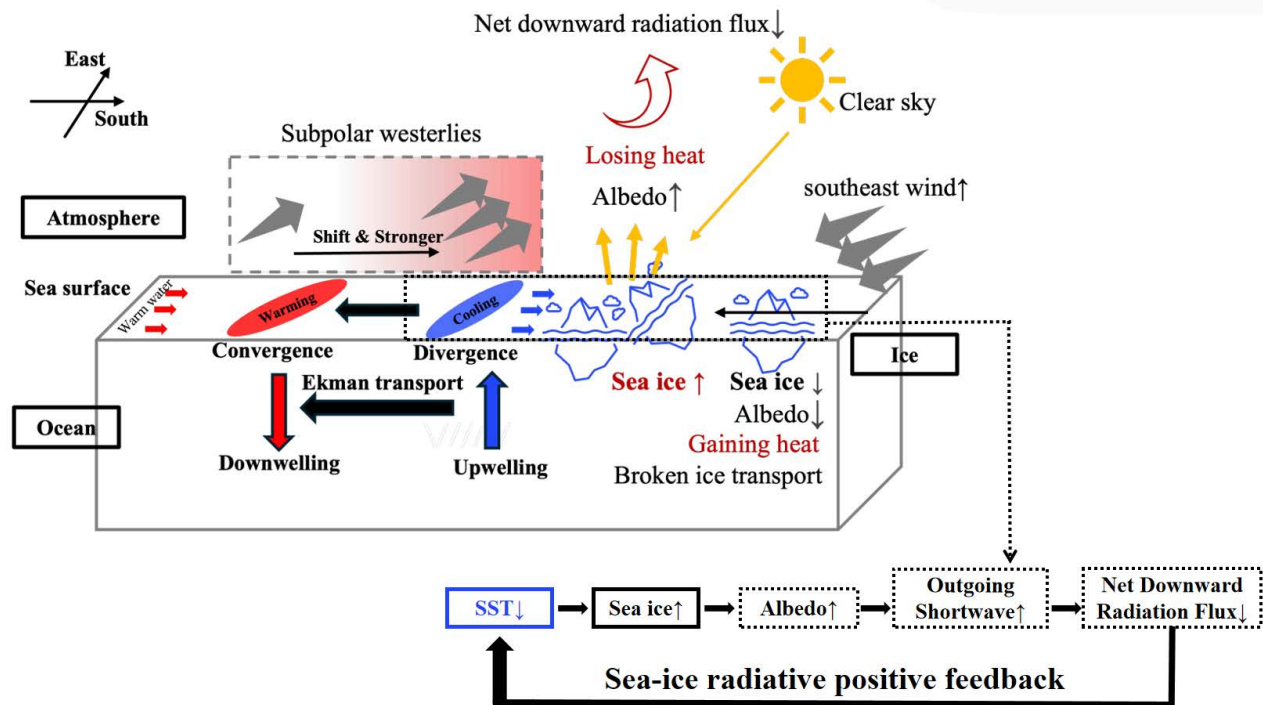


**Figure 7. Schematic diagram for contrasting SST trends in the southern pacific Ocean, illustrating the sea-ice-air interactions and sea ice radiative feedback.**

Data Availability Statement
The SST data product is available from https://doi. org/10.48670/moi-00243/. The SSH data is avail- able from: https://doi.org/10.48670/moi-00238/. Energy Balanced and Filled (EBAF) level-3 source is available from: https://ceres.larc.nasa.gov/data/#ebaftoa-level-3/. NCEP-NCAR Reanalysis 1 is avail- able from: https://psl.noaa. gov/. NSIDC is available at: https://nsidc.org/data/.

## References

[1] Bowen, M., Markham,J., Sutton, P., Zhang, X., Wu, Q., Shears, N. T., & Fernandez, D. (2017). Inter- annual Variability of Sea Surface Temperature in the Southwest Pacific and the Role of Ocean Dynamics. Journal of Climate, 30(18), 7481–7492. https://doi.org/10.1175/JCLI-D-16-0852.1

[2] Cushman-Roisin, B., & Beckers, J.-M. (2011). Chapter 8 - The Ekman Layer. In B. Cushman-Roisin & J.-M. Beckers (Eds.), Introduction to Geophysical Fluid Dynamics (Vol. 101, pp. 239–270). Academic Press. https://doi.org/10.1016/B978-0-12-088759-0.00008-0

[3] Fernandez, Denise, Bowen, Melissa, Sutton, & Philip. (2022). South Pacific Ocean Dynamics Redis- tribute Ocean Heat Content and Modulate Heat Exchange With the Atmosphere. Geophysical Research Letters, 49(23), e2022GL100965. https://doi.org/10.1029/2022GL100965

[4] Haumann, Alexander, F., Gruber, Nicolas, & Münnich, M. (2020). Sea-Ice Induced Southern Ocean Subsurface Warming and Surface Cooling in a Warming Climate. AGU Advances, 1(2), e2019AV000132. https://doi.org/10.1029/2019AV000132

[5] Hobbs, W. R., Massom, R., Stammerjohn, S., Reid, P., Williams, G., & Meier, W. (2016). A review of recent changes in Southern Ocean sea ice, their drivers and forcings. Global and Planetary Change, 143, 228–250. https://doi.org/https://doi.org/10.1016/j.gloplacha.2016.06.008

[6] Jones, R. N., & Ricketts,J. H. (2021). The Pacific Ocean heat engine. Earth System Dynamics Discus- sions, 1–47. https://api.semanticscholar.org/CorpusID:236783792

[7] Kalnay, E., Kanamitsu, M., Kistler, R. E., Collins,W. D., Deaven, D. G., Gandin, L. S., Iredell, M., Saha, S., White, G. H., Woollen,J. S., Zhu,Y., Chelliah, M., Ebisuzaki,W., Higgins,W.J., Janowiak,J. E., Mo, K. C., Ropelewski, C., Wang,J., Leetmaa, A., … Joseph, D. (1996). The NCEP/NCAR 40-Year Reanalysis

*Project. Renewable Energy. https://api.semanticscholar.org/ CorpusID:124135431*

*[8] Kato, S., Rose, F. G., Rutan, D. A., Thorsen, T. J., Loeb, N. G., Doelling, D. R., Huang, X., Smith, W. L., Su, W., & Ham, S.-H. (2018). Surface Irradiances of Edition 4.0 Clouds and the Earth's Radiant Energy System (CERES) Energy Balanced and Filled (EBAF) Data Product. Journal of Climate, 31(11), 4501– 4527. https://doi.org/10.1175/JCLI-D-17-0523.1*

*[9] Kieu, C. Q., Zhao, M., Tan, Z., Zhang, B., & Knutson, T. R. (2023). On the Role of Sea Surface Temperature in the Clustering of Global Tropical Cyclone Formation. Journal of Climate. https://api. semanticscholar.org/CorpusID:256294860*

*[10] Li,Q., Luo, Y., Lu,J., & Liu, F. (2022). The Role of Ocean Circulation in Southern Ocean Heat Uptake, Transport and Storage Response to Quadrupled CO2. Journal of Climate. https://api.semanticsc holar.org/CorpusID:251083035*

*[11] Loeb, N. G., Doelling, D. R., Wang, H., Su, W., Nguyen, C., Corbett, J. G., Liang, L., Mitrescu, C., Rose, F. G., & Kato, S. (2018). Clouds and the Earth's Radiant Energy System (CERES) Energy Balanced and Filled (EBAF) Top-of-Atmosphere (TOA) Edition-4.0 Data Product. Journal of Climate, 31(2), 895–918. https://doi.org/10.1175/JCLI-D-17-0208.1*

*[12] Meier, N., W., Fetterer, F., W., K., A., Stewart, & S., J. (2021). Near-Real-Time NOAA/NSIDC Climate Data Record of Passive Microwave Sea Ice Concentration, Version 2. https:// doi.org/10.7265/tgam-yv28*

*[13] Merchant, C.J., Embury, O., Bulgin, & C.E. (2019). Satellite-based time-series of sea-surface temperature since 1981 for climate applications. Sci Data, 6(223). https://doi. org/10.1038/s41597-019-0236-x*

*[14] Saurral, D.-R. F. &. G.-S. J., R.I. (2018). Observed modes of sea surface temperature variability in the South Pacific region. Clim Dyn, 50, 1129–1143. https://doi.org/10.1007/ s00382-017-3666-1*

*[15] Seager, R., Henderson,N., & Canea,M. (2022). Persistent Discrepancies between Observed and Modeled Trends in the Tropical Pacific Ocean. https://api.semanticscholar.org/ CorpusID:253501859*

*[16] Serratosa, J., Hyrenbach, K. D., Miranda-Urbina, D., Portflitt-Toro, M., Luna, N., & Luna-Jorquera, G. (2020). Environmental Drivers of Seabird At-Sea Distribution in the Eastern South Pacific Ocean: Assemblage Composition Across a Longitudinal Productivity Gradient. Frontiers in Marine Science, 6. https://doi.org/10.3389/fmars.2019.00838*

*[17] Sutton,H., P.J., Rickard,J., G., Roemmich, & H., D. (2024). Southwest Pacific Ocean Warming Driven by Circulation Changes. Geophysical Research Letters, 51(13), e2024GL109174. https://doi.org/10.1029/2024GL109174*

*[18] Turner, John, Holmes, Caroline, Harrison, C., Thomas, Phillips, Tony, Jena, Babula, Reeves-Francois, Tylei, Fogt, Ryan, Thomas, E. R., & Bajish, C. C. (2022). Record Low Antarctic Sea Ice Cover in February 2022. Geophysical Research Letters, 49(12), e2022GL098904. https://doi. org/10.1029/2022GL098904*

*[19] Xu, Xiaoqi,Liu, Jiping, Huang, & Gang. (2022). Understanding Sea Surface Temperature Cooling in the Central-East Pacific Sector of the Southern Ocean During 1982–2020. Geophysical Research Letters, 49(10), e2021GL097579. https:// doi.org/10.1029/2021GL097579*